Hindawi
Geofluids
Volume 2022, Article ID 5993701, 11 pages
https://doi.org/10.1155/2022/5993701

Research Article

Transient Pressure Behavior of a Horizontal Well in a Naturally Fractured Gas Reservoir with Dual-Permeability Flow and Stress Sensitivity Effect

Guiqin Wang, Rui Zhang, and Liangliang Cui

School of Petroleum and Environmental Engineering, Yan'an University, Yan'an 716000, China

Correspondence should be addressed to Guiqin Wang; guiqin1990@126.com

Received 28 February 2022; Accepted 11 April 2022; Published 30 April 2022

Academic Editor: Zheng Sun

Dual-permeability flow and stress sensitivity effect are two fundamental issues that have been widely investigated in transient pressure analysis for horizontal wells. However, few attempts have been made to simulate the combined effects of dual-permeability flow and stress-dependent fracture permeability on the pressure transient dynamics of a horizontal well in a naturally fractured gas reservoir. In this approach, an analytical model is proposed to integrate the complexities of pressure-dependent PVT properties, dual-permeability flow behavior, and stress-dependent fracture permeability characteristics. The nonlinearity of the mathematical model is weakened by using Pedrosa's transform formulation. Then, the Laplace integral transformation and separation of variables are applied to solve the model. Based on the solution of the mathematical model, a series of new-type curves are drawn to make a precise observation of different flow regimes. The main differences between the proposed model and the traditional models are discussed, and the effects of the permeability modulus of fractures, storability ratio, interporosity flow factor, and skin factor on transient pressure response are also examined. The results show that there are obvious differences in transient pressure dynamic curves between the proposed model and traditional models. The stress sensitivity effect plays a significant role in the intermediate flow period and the late-time pseudoradial flow period. The dual-permeability flow behavior mainly affects the early transient and interporosity flow stages. The proposed model can accurately simulate the transient pressure behaviors of a horizontal well in a naturally fractured gas reservoir with a dual-permeability flow and stress sensitivity effect. The novel model can be used to interpret pressure signals with accurate matching results and more reasonable interpreted parameters.

1. Introduction

Transient pressure analysis of a horizontal well in a naturally fractured gas reservoir is greatly affected by fracture seepage parameters and stress-dependent fracture permeability. For naturally fractured reservoirs, the fractures are always with heterogeneities [1, 2]. An experimental study on fracture stress sensitivities proves that stress-dependent fracture permeability significantly affects the transient pressure response [3]. So, it is pretty essential to propose a comprehensive model to capture the transient behavior of horizontal wells in naturally fractured gas reservoirs.

Because it is often impossible to describe the complex fractures precisely, continuum models are proposed to capture the flow behavior of this kind of reservoir. Much research has been done on theoretical models of vertical wells in naturally fractured reservoirs. Barenblatt et al. [4] proposed a classic double-porosity and single-permeability model to study vertical well production in porous media reservoirs. This model assumes that a naturally fractured reservoir is composed of two completely overlapping continua, porous matrix, and fractures. Warren and Root [5] expanded Barenblatt et al.'s approach to cover the independent physical properties of fracture and matrix. In their model, naturally fractured formation is formed by matrix blocks, which is separated by uniform and orthogonal fractures. Besides, the pseudosteady-state interporosity flow is firstly adopted to simulate mass transfer between fracture

and matrix systems. After that, Kazemi et al. [6], de Swaan [7], Raghavan and Ohaeri [8], Serra et al. [9], Jalali and Ershaghi [10], Wu and Pruess [11], Bui et al. [12], Wu et al. [13], Kuchuk et al. [14], Jia et al. [2], and Wang et al. [15] proposed their own dual-media model for naturally fractured reservoirs with the consideration of transient interporosity flow behavior. These models assume that the fracture system is the only flow pathway directly connected with wellbore by ignoring the flow from the matrix system to the wellbore. Because the dual-porosity and single-permeability model is no longer applicable in naturally fractured reservoirs, a great deal of work have instead been directed at using dual-porosity and dual-permeability models [14, 16–18] to describe the flow behavior, which assumes that both the fracture and matrix systems are the flow pathway directly connected with the wellbore, also considered the pseudosteady-state and transient-state interporosity flow between matrix and fracture systems. However, most of the models ignored the effect of the stress-dependent fracture permeability on transient pressure response. Although a great deal of work has been done on theoretical models of naturally fractured gas wells considering stress sensitivity of fracture permeability, most of them are restricted to the dual-porosity and single-permeability flow problem [3, 15, 19–21].

In recent years, horizontal wells have been increasingly applied to some naturally fractured gas reservoirs. Research on the transient pressure behavior of this kind of well has become increasingly popular among engineers [22–30]. However, transient pressure analysis for horizontal wells is commonly performed assuming that permeability for natural fractures remains constant, which might not be physically applicable for stress-sensitive reservoirs. Besides, dual-permeability flow is seldom considered in their models. In general, the big challenge of analyzing the transient pressure response of a horizontal well is that the dual-permeability flow behavior and stress-dependent fracture permeability should be all incorporated in the mathematical models.

This paper presented a novel semianalytical model to examine the combined effects of dual-permeability flow behavior and stress-dependent fracture permeability on the transient pressure response of a horizontal well in a naturally fractured gas reservoir. The nonlinearity of the governing equations caused by the stress sensitivity of fracture permeability is eliminated using Pedrosa's [31] transform formulation. With Laplace transform and separation of variables, we got the analytical solution of the mathematical model. A series of new transient pressure dynamic curves are drawn to observe different flow regimes based on the solution. Then, differences between the proposed model and traditional models are discussed and the effects of some critical parameters on transient pressure response are also analyzed with the proposed model.

2. Methodology

2.1. Model Assumption. As shown in Figure 1, the naturally fractured gas reservoir is composed of fracture and matrix systems and the physical properties of the two systems are independent. A radial cylindrical dual-porosity and dual-permeability medium reservoir is considered in which a single horizontal well is located at the center, completely penetrating the formation. The matrix/fracture flow is schematically described in Figure 2. In this study, the proposed model assumes that both the fracture and matrix systems are the flow pathway directly connected with the wellbore and fluids in the fracture and matrix systems first flow into the horizontal wellbore, followed by the matrix-fracture interporosity flow. Some simplifying physical model assumptions for the derivation of the governing equation are listed as the horizontal well produced with the constant production rate in a naturally fractured gas reservoir. The external boundaries of the top and bottom are assumed to be closed, and the lateral boundary is assumed to be infinite. The matrix-fracture interporosity flow in the reservoir is described by the pseudosteady-state model [5, 25, 26]. Fluid flow follows the law of Darcy seepage, and stress-dependent fracture permeability is considered. Also, capillary and gravity forces are neglected to simplify the model.

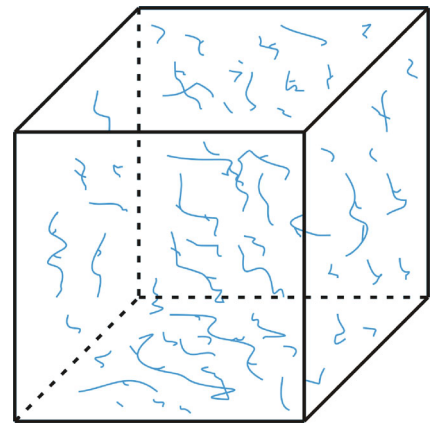

Figure 1: Schematic of naturally fractured reservoir.

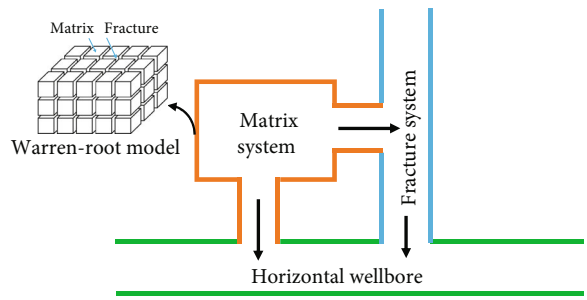

Figure 2: Dual-porosity and dual-permeability flow scheme.

2.2. Mathematical Model. The PVT properties, such as fluid viscosity and volume factor of the gas phase, are quite sensitive to formation pressure. In this section, the pseudopressure transformation is used to capture pressure-dependent PVT properties and reduce the nonlinearity of governing differential equations. The definitions of pseudopressure and pseudotime are given by

$$\psi_j = 2\int_0^p \frac{p}{\mu_g Z} dp, \quad j = f, m,$$
$$t_a = \int_0^t \frac{\mu_{gi} c_{ti}}{\mu_g(p) c_t(p)} dt, \tag{1}$$

where p is the pressure, MPa; ψ_f is the pseudopressure of the fracture, MPa^2/(mPa·s); ψ_m is the pseudo pressure of the matrix, MPa^2/(mPa·s); t is the time, h; t_a is the pseudotime; μ_g is the gas viscosity, mPa·s; c_t is the total compressibility coefficient, MPa^{-1}; and Z is the gas compressibility factor.

To describe the degree of stress sensitivity and its influence to fracture permeability, the concept of pseudopermeability modulus γ_f is defined as [19, 26]

$$\gamma_f = \frac{1}{k_f}\frac{\partial k_f}{\partial \psi_f}. \tag{2}$$

Equation (2) can be further written as

$$k_f = k_{fi} e^{-\gamma_f(\psi_i - \psi_f)}, \tag{3}$$

where k_f is the permeability of fracture, mD; k_{fi} is the initial permeability of fracture, mD; ψ_i is the initial pseudopressure, MPa^2/(mPa·s); and γ_f is the pseudopermeability modulus of the fracture, (mPa·s)/MPa^2.

To establish and solve the model, a radial cylindrical system (r) is used to describe the flow of the fracture and matrix system. With consideration of the dual-porosity and dual-permeability flow behavior and stress-dependent fracture permeability, the governing differential equation of the complex system can be described as follows:

For the fracture system,

$$\frac{\partial^2 \psi_f}{\partial r^2} + \frac{1}{r}\frac{\partial \psi_f}{\partial r} + \gamma_f\left(\frac{\partial \psi_f}{\partial r}\right)^2 + \frac{k_{fvi}}{k_{fhi}}\left[\frac{\partial^2 \psi_f}{\partial z^2} + \gamma_f\left(\frac{\partial \psi_f}{\partial z}\right)^2\right] + \alpha\frac{k_m}{k_{fhi}}\left(\psi_m - \psi_f\right) = e^{\gamma_f(\psi_i - \psi_f)}\frac{\phi_f \mu_g c_{tf}}{3.6 k_{fhi}}\frac{\partial \psi_f}{\partial t}. \tag{4}$$

For the matrix system,

$$\frac{\partial^2 \psi_m}{\partial r^2} + \frac{1}{r}\frac{\partial \psi_m}{\partial r} + \frac{k_{mv}}{k_{mh}}\frac{\partial^2 \psi_m}{\partial z^2} - \alpha\frac{k_m}{k_{mh}}\left(\psi_m - \psi_f\right) = \frac{\phi_m \mu_g c_{tm}}{3.6 k_{mh}}\frac{\partial \psi_m}{\partial t}. \tag{5}$$

For the initial condition,

$$\psi_f\Big|_{t=0} = \psi_m|_{t=0} = 0. \tag{6}$$

In the inner boundary condition,

$$\lim_{\varepsilon \to 0}\left[\lim_{r \to 0}\frac{4\pi h}{\mu_g \varepsilon}\int_{z_w - \varepsilon/2}^{z_w + \varepsilon/2}\left(k_{mh} r\frac{\partial \psi_m}{\partial r} + k_{fhi} e^{-\gamma_f(\psi_i - \psi_f)} r\frac{\partial \psi_f}{\partial r}\right) dz\right] = \frac{p_{sc} T Z}{p T_{sc}} q_{sc}, \ |z - z_w| \le \frac{\varepsilon}{2}. \tag{7}$$

The top and bottom boundaries are assumed to be closed and given by

$$\frac{\partial \psi_m}{\partial z}\Big|_{z=0} = \frac{\partial \psi_f}{\partial z}\Big|_{z=0} = 0,$$
$$\frac{\partial \psi_m}{\partial z}\Big|_{z=h} = \frac{\partial \psi_f}{\partial z}\Big|_{z=h} = 0 \tag{8}$$

The lateral boundary condition is assumed to be infinite and expressed as

$$\lim_{r \to \infty} \psi_m = \lim_{r \to \infty} \psi_f = \psi_i, \tag{9}$$

where c_{tf} is the total compressibility of the fracture, MPa^{-1}; c_{tm} is the total compressibility of the fracture, MPa^{-1}; h is the reservoir thickness, m; k_{fhi} is the initial horizontal permeability of the fracture, mD; k_{fvi} is the initial vertical permeability of the fracture, mD; k_{mh} is the horizontal permeability of the matrix, mD; k_{mv} is the vertical permeability of the matrix, mD; p is pressure, MPa; p_{sc} is the pressure at standard condition, MPa; q_{sc} is the surface gas production rate, 10^4 m^3/d; r is the radial distance, m; T is temperature, K; T_{sc} is the temperature at standard condition, K; z is the vertical distance from the bottom, m; z_w is the vertical distance of the horizontal well from the bottom, m; ε is a variable in the z direction, m; ϕ_f is the porosity of fracture; ϕ_m is the porosity of the matrix; and α is the geometric shape factor of matrix block, m^{-2}.

To make the equations homogeneous, some dimensionless variables are defined and tabulated in Table 1. Taking the dimensionless variables into equations (4)–(9), one can obtain the dimensionless differential equations.

For the fracture system,

$$\kappa\left\{\frac{\partial^2 \psi_{fD}}{\partial {r_D}^2} + \frac{1}{r_D}\frac{\partial \psi_{fD}}{\partial r_D} - \gamma_{fD}\left(\frac{\partial \psi_{fD}}{\partial r_D}\right)^2 + \frac{1}{h_D^2}\left[\frac{\partial^2 \psi_{fD}}{\partial {z_D}^2} - \gamma_{fD}\left(\frac{\partial \psi_{fD}}{\partial z_D}\right)^2\right]\right\} = e^{\gamma_{fD}\psi_{fD}}\left[\omega_f e^{-2S}\frac{\partial \psi_{fD}}{\partial t_D} + \lambda_{mf} e^{-2S}\left(\psi_{fD} - \psi_{mD}\right)\right]. \tag{10}$$

Table 1: Definitions of the parameters used in this work.

Parameters	Symbol	Definition
Dimensionless pseudopressure of the fracture	ψ_{fD}	$\psi_{fD} = \left(\left(78.489\left(k_{mh} + k_{fhi}\right)h\right)/Tq_{sc}\right)\left(\psi_i - \psi_f\right)$
Dimensionless pseudopressure of the matrix	ψ_{mD}	$\psi_{mD} = \left(\left(78.489\left(k_{mh} + k_{fhi}\right)h\right)/Tq_{sc}\right)\left(\psi_i - \psi_m\right)$
Dimensionless vertical distance	z_D	$z_D = z/h$
Dimensionless pseudotime	t_D	$t_D = \left(\left(3.6\left(k_{mh} + k_{fhi}\right)\right)/\left(\mu r_w{}^2\left(\phi_m C_{mt} + \phi_f C_{\mathrm{ft}}\right)\right)\right)t_a$
Dimensionless reservoir thickness	h_D	$h_D = \left(h/r_w e^{-S}\right)\sqrt{\left(k_{fhi}/k_{fpi}\right)}$
Dimensionless radial distance	r_D	$r_D = r/r_w e^{-S}$
Dimensionless wellbore storage coefficient	C_D	$C_D = C_s/\left(6.2832\left(\phi_f C_{\mathrm{ft}} + \phi_m C_{mt}\right)hr_w^2\right)$
Dimensionless pseudopermeability modulus	γ_{fD}	$\gamma_{fD} = \left(Tq_{sc}/78.489k_{fhi}h\right)\gamma_f$
The permeability ratio of the fracture system to the sum of the fracture and matrix system	κ	$\kappa = k_{fhi}/\left(k_{fhi} + k_{mh}\right)$
Capacitance coefficient of the fracture	ω_f	$\omega_f = \phi_f C_{\mathrm{ft}}/\left(\phi_f C_{\mathrm{ft}} + \phi_m C_{mt}\right)$
Interporosity flow factor of matrix system into the fracture system	λ_{mf}	$\lambda_{mf} = \alpha_m k_{mh} r_w^2/\left(k_{fhi} + k_{mh}\right)$

For the matrix system,

$$(1-\kappa)\left(\frac{\partial^2\psi_{mD}}{\partial r_D{}^2} + \frac{1}{r_D}\frac{\partial\psi_{mD}}{\partial r_D} + \frac{1}{h_D^2}\frac{\partial^2\psi_{mD}}{\partial z_D{}^2}\right) - \lambda_{mf}e^{-2S}\left(\psi_{mD} - \psi_{fD}\right) = \omega_m e^{-2S}\frac{\partial\psi_{mD}}{\partial t_D}. \tag{11}$$

In the initial condition,

$$\psi_{fD}\Big|_{t_D=0} = \psi_{mD}\big|_{t_D=0} = 0. \tag{12}$$

In the inner boundary condition,

$$\lim_{\varepsilon_D\longrightarrow 0}\left[\lim_{r_D\longrightarrow 0}\int_{z_{wD}-(\varepsilon_D/2)}^{z_{wD}+(\varepsilon_D/2)}\left(\kappa r_D\frac{\partial\psi_{mD}}{\partial r_D} + (1-\kappa)r_D e^{-\gamma_{fD}\psi_{fD}}\frac{\partial\psi_{fD}}{\partial r_D}\right)dz_D\right] = -\frac{1}{2}, \left|z_D - z_{wD}\right| \le \frac{\varepsilon_D}{2}. \tag{13}$$

In the outer boundary conditions,

$$\frac{\partial\psi_{mD}}{\partial z_D}\Big|_{z_D=0} = \frac{\partial\psi_{fD}}{\partial z_D}\Big|_{z_D=0} = 0, \tag{14}$$

$$\frac{\partial\psi_{mD}}{\partial z_D}\Big|_{z_D=1} = \frac{\partial\psi_{fD}}{\partial z_D}\Big|_{z_D=1} = 0, \tag{15}$$

$$\lim_{r_D\longrightarrow\infty}\psi_{mD} = \lim_{r_D\longrightarrow\infty}\psi_{fD} = 0. \tag{16}$$

2.3. Solution to the Mathematical Model. It should be noted that equations (10) and (13) are strongly nonlinear with the consideration of the stress sensitivity of fracture permeability. This is because the stress-dependent fracture permeability is a function of the pseudopressure of the fracture. However, the pressure of fracture is an unknown parameter. Therefore, the mathematical model cannot be solved analytically. In this work, the Pedrosa [31] variable substitution and regular perturbation method are firstly deployed to alleviate the nonlinearity. Then, the Laplace transformation and separation of variables are adopted to address the linearized model. Thus, the model can be solved in the Laplace space and the Stehfest and Harald [32] numerical inversion is used to calculate the pressure in real space.

2.3.1. Linearization of the Flow Equation. To linearize the mathematical model, the Pedrosa transformation is employed in this section and given by

$$\psi_{fD}(r_D, t_D)\Big|_{t_D=0} = -\frac{1}{\gamma_{fD}}\ln\left[1 - \gamma_{fD}\eta_{fD}(r_D, t_D)\right], \tag{17}$$

where η_{fD} is an intermediate variable called the perturbation deformation function.

After the Pedrosa transformation, equations (10)–(16) can be rewritten as

$$\kappa\left(\frac{\partial^2\eta_{fD}}{\partial r_D{}^2} + \frac{1}{r_D}\frac{\partial\eta_{fD}}{\partial r_D} + \frac{1}{h_D^2}\frac{\partial^2\eta_{fD}}{\partial z_D{}^2}\right) = e^{-2S}\left[\frac{1}{1-\gamma_{fD}\eta_{fD}}\omega_f\frac{\partial\eta_{fD}}{\partial t_D} + \left(1-\omega_f\right)\frac{\partial\psi_{mD}}{\partial t_D}\right], \tag{18}$$

$$(1-\kappa)\left(\frac{\partial^2\psi_{mD}}{\partial r_D{}^2} + \frac{1}{r_D}\frac{\partial\psi_{mD}}{\partial r_D} + \frac{1}{h_D^2}\frac{\partial^2\psi_{mD}}{\partial z_D{}^2}\right) = e^{-2S}\left\{\left(1-\omega_f\right)\frac{\partial\psi_{mD}}{\partial t_D} + \lambda_{mf}\left[\frac{1}{\gamma_{fD}}\ln\left(1-\gamma_{fD}\eta_{fD}\right) - \psi_{mD}\right]\right\}, \tag{19}$$

$$\eta_{fD}(r_D, t_D)\Big|_{t_D=0} = \psi_{mD}(r_D, t_D)|_{t_D=0} = 0, \tag{20}$$

$$\lim_{\varepsilon_D \longrightarrow 0}\left[\lim_{r_D \longrightarrow 0}\int_{z_{wD}-(\varepsilon_D/2)}^{z_{wD}+(\varepsilon_D/2)}\left((1-\kappa)r_D\frac{\partial\psi_{mD}}{\partial r_D} + \kappa r_D\frac{\partial\eta_{fD}}{\partial r_D}\right)dz_D\right] = -\frac{1}{2}, |z_D - z_{wD}| \le \frac{\varepsilon_D}{2}, \tag{21}$$

$$\frac{\partial\eta_{fD}}{\partial z_D}\Big|_{z_D=1} = \frac{\partial\psi_{mD}}{\partial z_D}\Big|_{z_D=1} = 0, \tag{22}$$

$$\frac{\partial\eta_{fD}}{\partial z_D}\Big|_{z_D=0} = \frac{\partial\psi_{mD}}{\partial z_D}\Big|_{z_D=0} = 0, \tag{23}$$

$$\lim_{r_D \longrightarrow \infty}\psi_{mD} = \lim_{r_D \longrightarrow \infty}\eta_{fD} = 0. \tag{24}$$

According to the regular perturbation theory, equations (18)–(24) can be simplified as

$$\kappa\left(\frac{\partial^2\eta_{fD0}}{\partial {r_D}^2} + \frac{1}{r_D}\frac{\partial\eta_{fD0}}{\partial r_D} + \frac{1}{h_D^2}\frac{\partial^2\eta_{fD0}}{\partial {z_D}^2}\right) = \left[\omega_f e^{-2S}\frac{\partial\eta_{fD0}}{\partial t_D} + \lambda_{mf}e^{-2S}\left(\eta_{fD0} - \psi_{mD}\right)\right], \tag{25}$$

$$(1-\kappa)\left(\frac{\partial^2\psi_{mD}}{\partial {r_D}^2} + \frac{1}{r_D}\frac{\partial\psi_{mD}}{\partial r_D} + \frac{1}{h_D^2}\frac{\partial^2\psi_{mD}}{\partial {z_D}^2}\right) = \left(1-\omega_f\right)e^{-2S}\frac{\partial\psi_{mD}}{\partial t_D} + \lambda_{mf}e^{-2S}\left(\eta_{fD0} - \psi_{mD}\right), \tag{26}$$

$$\eta_{fD0}(r_D, t_D)\Big|_{t_D=0} = \psi_{mD}(r_D, t_D)|_{t_D=0} = 0, \tag{27}$$

$$\lim_{\varepsilon_D \longrightarrow 0}\left[\lim_{r_D \longrightarrow 0}\int_{z_{wD}-(\varepsilon_D/2)}^{z_{wD}+(\varepsilon_D/2)}\left((1-\kappa)r_D\frac{\partial\psi_{mD}}{\partial r_D} + \kappa r_D\frac{\partial\eta_{fD0}}{\partial r_D}\right)dz_D\right] = -\frac{1}{2}, |z_D - z_{wD}| \le \frac{\varepsilon_D}{2}, \tag{28}$$

$$\frac{\partial\eta_{fD0}}{\partial z_D}\Big|_{z_D=1} = \frac{\partial\psi_{mD}}{\partial z_D}\Big|_{z_D=1} = 0, \tag{29}$$

$$\frac{\partial\eta_{fD0}}{\partial z_D}\Big|_{z_D=0} = \frac{\partial\psi_{mD}}{\partial z_D}\Big|_{z_D=0} = 0, \tag{30}$$

$$\lim_{r_D \longrightarrow \infty}\psi_{mD} = \lim_{r_D \longrightarrow \infty}\eta_{fD0} = 0. \tag{31}$$

2.3.2. Solution of the Proposed Model. To derive the analytical solution of the model, the mathematical model is translated into the Laplace domain with respect to t_D:

$$L\left[\eta_{fD}(r_D, t_D)\right] = \bar{\eta}_{fD}(r_D, u) = \int_0^{+\infty}\eta_{fD}(r_D, t_D)e^{-ut_D}dt_D, \tag{32}$$

$$L[\psi_{mD}(r_D, t_D)] = \bar{\psi}_{mD}(r_D, u) = \int_0^{+\infty}\psi_{mD}(r_D, t_D)e^{-ut_D}dt_D, \tag{33}$$

where u is the Laplace transform variable.

With equations (32) and (33) and taking the Laplace transform of equations (25)–(31), one can obtain the dimensionless mathematical model in the Laplace space:

For the fracture system,

$$\frac{\partial^2\bar{\eta}_{fD}}{\partial {r_D}^2} + \frac{1}{r_D}\frac{\partial\bar{\eta}_{fD}}{\partial r_D} + \frac{1}{h_D^2}\frac{\partial^2\bar{\eta}_{fD}}{\partial {z_D}^2} + \frac{A_1}{\kappa}\bar{\eta}_{fD} + \frac{A_2}{\kappa}\bar{\psi}_{mD} = 0. \tag{34}$$

For the matrix system,

$$\frac{\partial^2\bar{\psi}_{mD}}{\partial {r_D}^2} + \frac{1}{r_D}\frac{\partial\bar{\psi}_{mD}}{\partial r_D} + \frac{1}{h_D^2}\frac{\partial^2\bar{\psi}_{mD}}{\partial {z_D}^2} + \frac{A_2}{1-\kappa}\bar{\eta}_{fD} + \frac{A_3}{1-\kappa}\bar{\psi}_{mD} = 0, \tag{35}$$

where $A_1 = -(\lambda_{mf} + u\omega_f)e^{-2S}$, $A_2 = \lambda_{mf}e^{-2S}$, and $A_3 = -[\lambda_{mf} + u(1-\omega_f)]e^{-2S}$.

In the inner boundary condition,

$$\lim_{\varepsilon_D \longrightarrow 0}\left[\lim_{r_D \longrightarrow 0}\int_{z_{wD}-(\varepsilon_D/2)}^{z_{wD}+(\varepsilon_D/2)}\left((1-\kappa)r_D\frac{\partial\bar{\psi}_{mD}}{\partial r_D} + \kappa r_D\frac{\partial\bar{\eta}_{fD0}}{\partial r_D}\right)dz_D\right] = -\frac{1}{2u}, |z_D - z_{wD}| \le \frac{\varepsilon_D}{2}. \tag{36}$$

In the outer boundary conditions,

$$\frac{\partial\bar{\psi}_{mD}}{\partial z_D}\Big|_{z_D=0} = \frac{\partial\bar{\eta}_{fD0}}{\partial z_D}\Big|_{z_D=0} = 0, \tag{37}$$

$$\frac{\partial\bar{\psi}_{mD}}{\partial z_D}\Big|_{z_D=1} = \frac{\partial\bar{\eta}_{fD0}}{\partial z_D}\Big|_{z_D=1} = 0, \tag{38}$$

$$\lim_{r_D \longrightarrow \infty}\bar{\psi}_{mD} = \lim_{r_D \longrightarrow \infty}\bar{\eta}_{fD0} = 0. \tag{39}$$

This section uses the separation of variables to solve the dual-porosity and dual-permeability modeling of a horizontal well in a naturally fractured reservoir. With the separation of variables, the dimensionless pseudopressure in the Laplace space can be separated by [25]

$$\bar{\eta}_{jD} = \bar{R}_j(r_D)\bar{Z}_j(z_D), \quad j = m, f. \tag{40}$$

Substituting equation (40) into equations (34) and (35), one can obtain

$$\frac{h_{\mathrm{D}}^2\left(\bar{R}_{\mathrm{j}}'' + (1/r_{\mathrm{D}})\bar{R}_{\mathrm{j}}' - \sigma\bar{R}_{\mathrm{j}}\right)}{\bar{R}_{\mathrm{j}}} = -\frac{\bar{Z}_{\mathrm{j}}''}{\bar{Z}_{\mathrm{j}}} = \lambda. \tag{41}$$

According to equation (41), the fluid flow in the horizontal direction can be written as

$$\bar{R}_{\mathrm{j}}'' + \frac{1}{r_{\mathrm{D}}}\bar{R}_{\mathrm{j}}' - \xi\bar{R}_{\mathrm{j}} = 0, \tag{42}$$

$$\xi = \sigma + \frac{\lambda}{h_D^2}. \tag{43}$$

And the fluid flow in the vertical direction is

$$\bar{Z}_j'' + \lambda\bar{Z}_j = 0. \tag{44}$$

Without consideration of the flow in the z-direction and taking equation (42) into equations (34) and (35), we have

$$\frac{\partial^2\bar{R}_{fD}}{\partial {r_D}^2} + \frac{1}{r_D}\frac{\partial\bar{R}_{fD}}{\partial r_D} + \frac{A_1}{\kappa}\bar{R}_{fD} + \frac{A_2}{\kappa}\bar{R}_{mD} = 0, \tag{45}$$

$$\frac{\partial^2\bar{R}_{mD}}{\partial {r_D}^2} + \frac{1}{r_D}\frac{\partial\bar{R}_{mD}}{\partial r_D} + \frac{A_2}{(1-\kappa)}\bar{R}_{fD} + \frac{A_3}{(1-\kappa)}\bar{R}_{mD} = 0. \tag{46}$$

Under the infinite external boundary of side, the solutions of equations (45) and (46) can be expressed by

$$\bar{R}_f = A_f K_0\left(\sqrt{\sigma}r_D\right), \tag{47}$$

$$\bar{R}_m = A_m K_0\left(\sqrt{\sigma}r_D\right). \tag{48}$$

Substituting equations (47) and (48) into (45) and (46), we have

$$\sigma K_0\left(\sqrt{\sigma}r_D\right)A_f + \frac{A_1}{\kappa}K_0\left(\sqrt{\sigma}r_D\right)A_f + \frac{A_2}{\kappa}K_0\left(\sqrt{\sigma}r_D\right)A_m = 0, \tag{49}$$

$$\begin{aligned}\sigma K_0\left(\sqrt{\sigma}r_D\right)A_m + \frac{A_2}{1-\kappa}K_0\left(\sqrt{\sigma}r_D\right)A_f \\ + \frac{A_3}{1-\kappa}K_0\left(\sqrt{\sigma}r_D\right)A_m = 0.\end{aligned} \tag{50}$$

Because the modeling must have solutions, the coefficients A_m and A_f cannot be zero, so the term σ in equation (50) can be given by

$$\sigma = \frac{-[\kappa A_3 + (1-\kappa)A_1] \pm \sqrt{[\kappa A_3 + (1-\kappa)A_1]^2 - 4\kappa(1-\kappa)\left(A_1A_3 - A_2^2\right)}}{2\kappa(1-\kappa)}. \tag{51}$$

With equation (49)–(51), the general solutions of equations (45) and (46) can be expressed by

$$\bar{R}_f = A_{f,1}K_0(\sqrt{\sigma_1}r_D) + A_{f,2}K_0(\sqrt{\sigma_2}r_D), \tag{52}$$

$$\bar{R}_m = A_{m,1}K_0(\sqrt{\sigma_1}r_D) + A_{m,2}K_0(\sqrt{\sigma_2}r_D), \tag{53}$$

$$\begin{aligned}A_{m,1} &= a_1A_{f,1}, \\ A_{m,2} &= a_2A_{f,2},\end{aligned} \tag{54}$$

$$\begin{aligned}a_1 &= -\frac{\kappa\sigma_1 + A_1}{A_2}, \\ a_2 &= -\frac{\kappa\sigma_2 + A_1}{A_2}.\end{aligned} \tag{55}$$

Considering the fluid flow in the z-direction, the general solutions of equations (52) and (53) can be given as

$$\bar{R}_f = A_{f,1}K_0\left(\sqrt{\xi_1}r_D\right) + A_{f,2}K_0\left(\sqrt{\xi_2}r_D\right), \tag{56}$$

$$R_m = a_1A_{f,1}K_0\left(\sqrt{\xi_1}r_D\right) + a_2A_{f,2}K_0\left(\sqrt{\xi_2}r_D\right), \tag{57}$$

$$\xi_1 = \sigma_1 + \frac{\lambda}{h_D^2}, \xi_2 = \sigma_2 + \frac{\lambda}{h_D^2}. \tag{58}$$

Combined with the boundary conditions, the terms $A_{f,1}$ and $A_{f,2}$ in equation (56) are

$$\begin{aligned}A_{f,2} &= \frac{1}{u}\frac{(1-a_1)K_0\left(\sqrt{\xi_1}\right)}{[\kappa + (1-\kappa)a_2](1-a_1)K_0\left(\sqrt{\xi_1}\right) - [\kappa + (1-\kappa)a_1](1-a_2)K_0\left(\sqrt{\xi_2}\right)}, \\ A_{f,1} &= \frac{1}{[\kappa + (1-\kappa)a_1]u} - \frac{\kappa + (1-\kappa)a_2}{\kappa + (1-\kappa)a_1}A_{f,2}.\end{aligned} \tag{59}$$

The general solution of equation (44) can be expressed by

$$\bar{Z}_j = C\cos\left(\sqrt{\lambda}z_D\right) + D\sin\left(\sqrt{\lambda}z_D\right). \tag{60}$$

Substituting equation (60) into equations (37) and (38), we have

$$\begin{aligned}&D = 0, \lambda = \lambda_n = (n\pi)^2, \quad n = 0, 1, 2, \cdots, \\ &C = \frac{1}{2}\cos\left(\sqrt{\lambda_n}z_{wD}\right), \lambda_n = (n\pi)^2, \quad n = 0, 1, 2, \cdots,\end{aligned} \tag{61}$$

so the solution in the vertical direction is

$$\bar{Z}_j = \frac{1}{2}\cos\left(\sqrt{\lambda}z_{wD}\right)\cos\left(\sqrt{\lambda}z_D\right). \tag{62}$$

Combined with equations (56), (57), and (62), the pressure solution for a three-dimensional volumetric source can be obtained and expressed by

$$\bar{\eta}_{fD} = \sum_{n=0}^{\infty}\bar{R}_{fn}\cdot\bar{Z}_{fn}. \tag{63}$$

According to the superposition principle, the dimensionless pressure in the Laplace space for constant-rate production can be obtained by integrating equation (63) along with the direction of horizontal wellbore.

$$\bar{\eta}_{sD} = \sum_{n=0}^{\infty} \int_{-L/2/r_w}^{L/2/r_w} \bar{R}_{fn} dx_D \cdot \bar{Z}_w. \tag{64}$$

Equation (64) is the dimensionless pseudopressure solution expression considering the skin effect. The wellbore storage effect can be incorporated in the abovementioned solution using Duhamel's principle [25], and the bottom-hole pressure solution is

$$\bar{\eta}_{wD} = \frac{\bar{\eta}_{sD}}{1 + C_D u^2 \bar{\eta}_{sD}}. \tag{65}$$

$\bar{\eta}_{wD}$ in equation (65) is the dimensionless pressure solution in the Laplace space, and in real space, the dimensionless pressure η_{wD} can be obtained using Stehfest numerical inversion [32]. After that, utilizing the inverse transformation of equation (66), the bottom-hole pressure response for a horizontal well incorporating the stress-dependent permeability of fracture system can be obtained:

$$\psi_{wD}(r_D, t_D) = -\frac{1}{\gamma_{fD}} \ln \left[1 - \gamma_{fD} \eta_{wD}(r_D, t_D)\right]. \tag{66}$$

3. New-Type Curves

In this work, a novel semi-analytical model is presented to examine the combined effects of dual-permeability flow behavior and stress-dependent fracture permeability on the transient pressure response of a horizontal well in a naturally fractured gas reservoir. A series of new transient pressure dynamic curves are drawn to observe different flow regimes based on the solution of the proposed model. The differences between the proposed model and traditional models are discussed, and the effects of some critical parameters on transient pressure response are also analyzed with the proposed model. Furthermore, it provides an efficient method for field engineers and related research and further to interpret pressure signals with accurate matching results and more reasonable interpreted parameters. After that, the effects of some critical parameters, including the dimensionless permeability modulus, the storability ratio of fracture, interporosity flow factor of matrix system into fracture system, and skin factor, on the characteristics of the type curves are examined and analyzed.

3.1. Flow Regime Identification. Figure 3 depicts the standard-type curves of wellbore pressure responses for a horizontal well located at a naturally fractured gas reservoir considering dual-permeability flow and stress-dependent fracture permeability. Basic data used to generate the type curves are listed in Table 2. An entire transient flow process is clearly shown, and the following six main flow stages can be recognized:

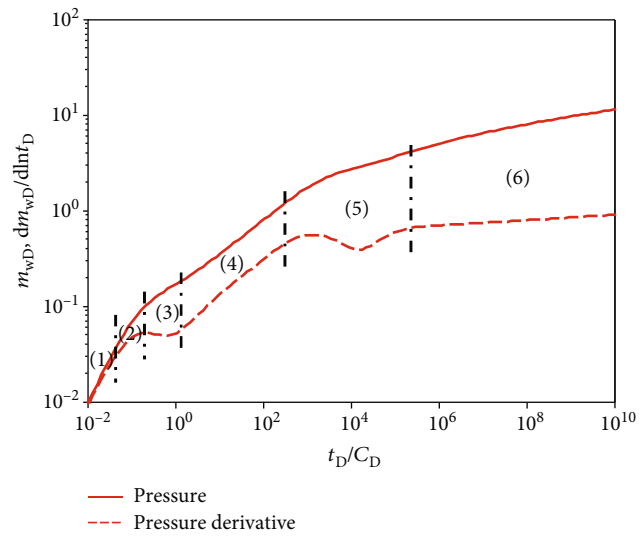

Figure 3: The transient responses with the log-log plot.

Table 2: Parameters used for model validation.

Parameters	Symbol	Value
Dimensionless wellbore storage coefficient	C_D	1×10^{-4}
Skin factor	S	0.1
Dimensionless reservoir thickness	h_D	400
Dimensionless horizontal section position	z_{wD}	0.5
Dimensionless pseudopermeability modulus	γ_{fD}	0.08
The permeability ratio of the fracture system to the sum of the fracture and matrix system	κ	0.9
Capacitance coefficient of the fracture	ω_f	0.05
Interporosity flow factor of the matrix system into the fracture system	λ_{mf}	0.01

(1) Pure wellbore storage stage: this period is characterized by a slope of 1 on the pressure and pressure derivative curves and governed by the wellbore storage coefficient, C

(2) Skin effect transition stage: the pressure derivative curve exhibits like a "hump." The peak of the "hump" is dominated by the skin factor, S

(3) Early radial flow stage: this period is present whenever the wellbore storage coefficient, C, and the horizontal wellbore length, L, are suitable. During this period, the pressure derivative curve is a horizontal line with a value of "$1/(4L_D)$"

(4) Early linear flow stage: it can be identified by a half-slope trend on the pressure derivative curve. During this period, gas flows linearly from the formation to natural fractures

(5) Interporosity flow stage from the matrix system to the fracture system: this process is characterized by a concave in the pressure derivative curve. The

concave shape is controlled by the storability ratio of fracture, ω_f, and the interporosity flow coefficient from the matrix system to the fracture system, λ_{mf}

(6) External boundary response stage: during this period, the pressures in the matrix and fracture systems reach a dynamic balance state. This period is marked by a slope of 0.5 on the pressure derivative curve without considering stress-dependent fracture permeability. However, the pressure derivative curve is no longer a horizontal line with a value of "0.5" but exhibits an upward tendency due to the effect of stress-dependent fracture permeability

3.2. Comparisons with the Traditional Models. So far, few attempts have been made to quantify the combined effects of dual-permeability flow behavior and stress-dependent fracture permeability on the transient pressure behavior of a horizontal well in fractured gas reservoirs. The main difference between the proposed and traditional models [25, 26] is that the dual-permeability flow behavior and stress-dependent fracture permeability are all incorporated in the new model. In this section, we simultaneously simulated the pressure response of both the proposed and conventional models using the same group of formation and well parameters in Table 2.

Figure 4 shows the comparison results of transient responses for the new model with the solution presented by Nie et al. [25]. The main difference between the two models is that stress-dependent fracture permeability is not considered in the model of Nie et al. [25]. As shown in Figure 4, fracture permeability stress sensitivity is found to significantly affect the middle stream flow period and the late-time pseudoradial flow period. There exist obvious differences during late-time pseudoradial flow period. The dimensionless pressure derivative curve exhibits a horizontal line with a value of 0.5 in the model of Nie et al. [25]; however, the derivative curve is no longer horizontal but bends upward in the new model. In addition, the location of the dimensionless pressure and pressure derivative curves during the middle stream flow period is higher in our model. This is because an additional pressure drop will be required to maintain a constant flow rate when the stress-sensitivity effect is taken into account.

We also compared the proposed model with the solution of a single-permeability model [26] based on the same reservoir properties and fracture parameters. The stress-dependent fracture permeability is considered both in two models. As can be seen in Figure 5, the combined effects of dual-permeability flow behavior and stress-dependent fracture permeability play a significant role in the early radial flow stage, the early linear flow stage, and the interporosity flow stage of the matrix system to the fracture system. Dimensionless pressure of the proposed model is lower than that of the single-permeability model [26] during the three flow periods. Besides, the concave in the pressure derivative curve of the dual-permeability model is shallower than that of single-permeability model. This is because the single-permeability model assumes that the fracture system is the only flow pathway directly connected with wellbore; however, the fluid supply from the matrix system to the wellbore is not considered. The dual-permeability flow behavior will accelerate energy supplement in the matrix during production compared with the single-permeability model.

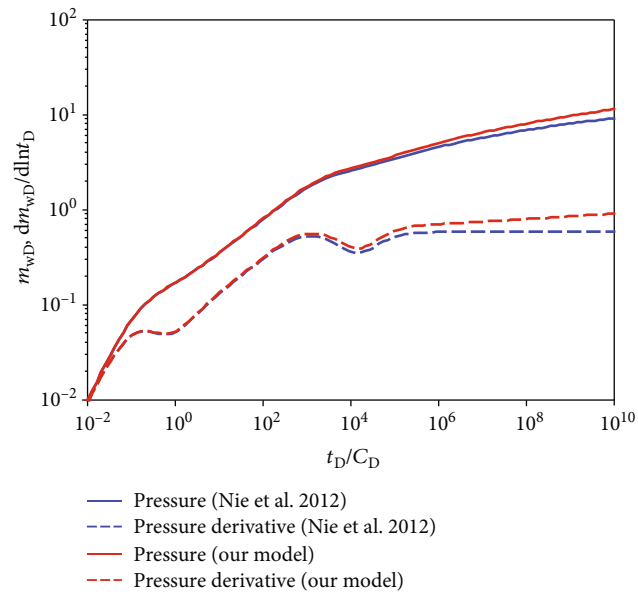

Figure 4: Comparison of the results of the proposed model with that of Nie et al. [25].

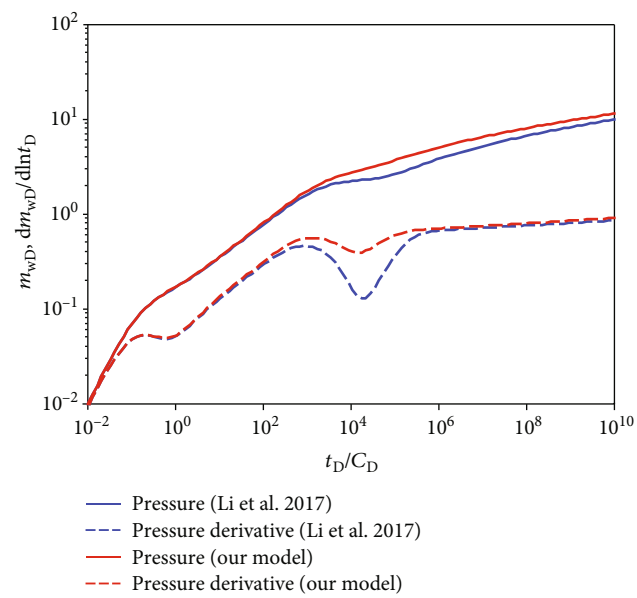

Figure 5: Comparison of the results of the proposed model with that of Li et al. [26].

3.3. Sensitivity Analysis. Based on the proposed model, the influences of stress sensitivity of fracture permeability, storativity ratio of the fracture, interporosity flow factor, and skin factor on pressure response are discussed. Except for the parameters analyzed, other parameters are the same and are shown in Table 2.

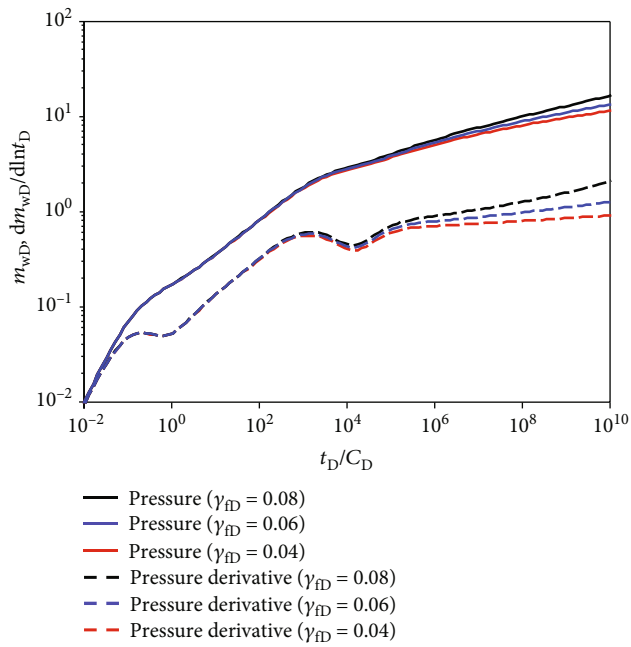

Figure 6: Effect of dimensionless permeability modulus, γ_{fD}, on type curves.

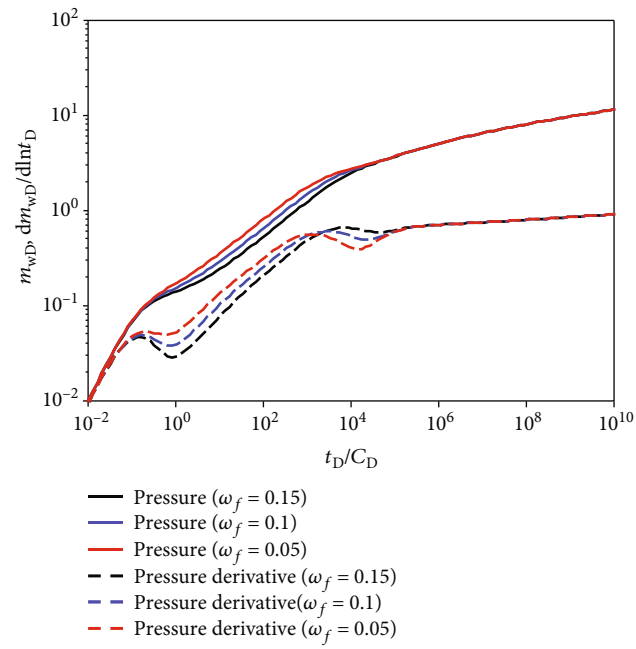

Figure 7: Effect of the storability ratio of the fracture, ω_f, on type curves.

3.3.1. Effect of the Permeability Modulus of the Fracture. The stress-sensitivity effect can be determined with the dimensionless permeability modulus, γ_{fD}. Figure 6 shows the pressure and pressure derivative curves for $\gamma_{fD} = 0.04$, 0.06, and 0.08. As stated, with increasing the value of γ_{fD}, the slope of the derivative curves increases during the intermediate and late time period. This is because the pressure drop increases as the dimensionless permeability modulus increases and fluid flow will be difficult and more gas is left in the reservoir. The stress sensitivity reflects the damage of permeability, and a larger dimensionless permeability modulus will increase the damage of permeability. Consequently, the permeability stress sensitivity of the fracture decreases the cumulative production. So, it is believed that reasonable producing pressure differential is excellent for reducing the negative effect of stress sensitivity on gas productivity in the development of fractured gas reservoirs.

3.3.2. Effect of the Storability Ratio of the Fracture. The effect of the storability ratio of the fracture, ω_f, on transient behavior is shown in Figure 7. As shown in Figure 7, the storability ratio of the fracture not only determines the duration and the depth of the concave but also has a significant effect on the early flow regimes (early radial and early linear flow stage). It can be clearly observed that the larger the ω_f is, the deeper and wider the concave in dimensionless pressure derivative curve. In addition, the dimensionless pressure curve becomes higher with the increase of the storability ratio of the fracture. This is because the storativity ratio of fracture reflects the relative capacity of fluid stored in the fracture system; a smaller storability ratio of the fracture is the response of relative abundant reserves in the matrix system. The pressure drop should increase to maintain the constant production rate when increasing the storability ratio of the fracture.

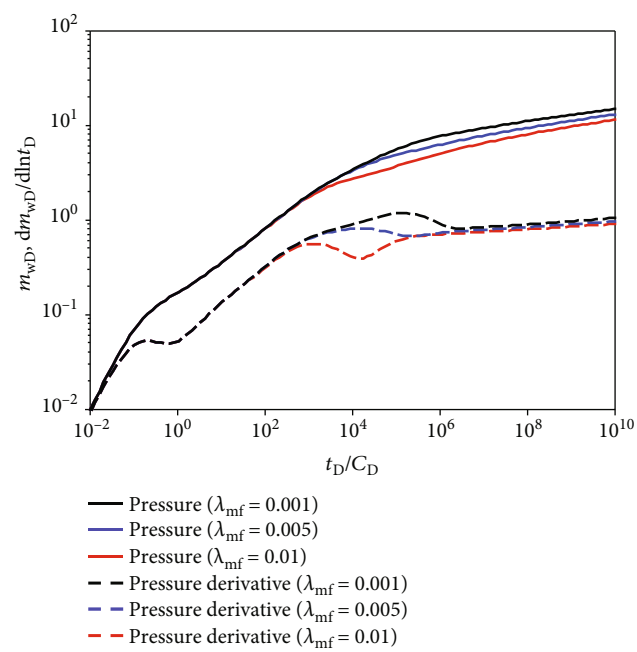

Figure 8: Effect of the interporosity flow factor, λ_{mf}, on type curves.

3.3.3. Effect of the Interporosity Flow Factor. The effect of the interporosity flow factor of the matrix system to the fracture system, λ_{mf}, on pressure response is shown in Figure 8. According to the definition of the interporosity flow factor,

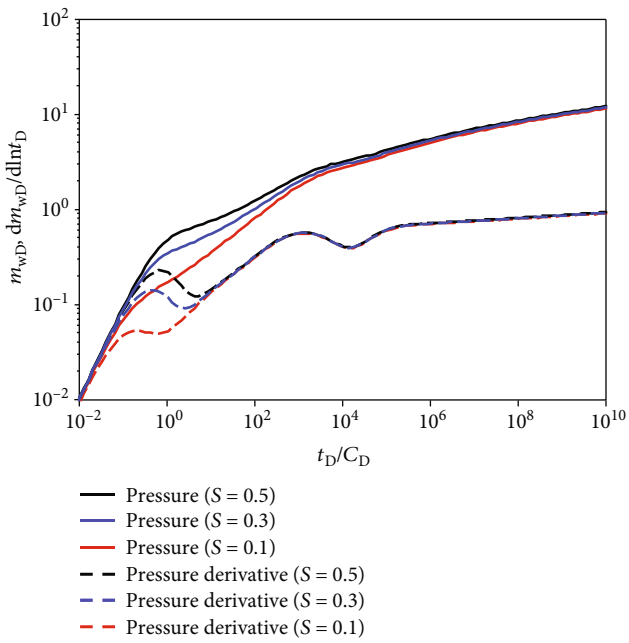

Figure 9: Effect of skin factor, S, on type curves.

the λ_{mf} represents the starting time of the flow exchange from the matrix system to the fracture system. The larger the λ_{mf} is, the earlier the time of the interporosity flow period is. Besides, the late-time pseudoradial flow period would be masked if the λ_{mf} is large enough.

3.3.4. Effect of the Skin Factor. The effect of the skin factor, S, on pressure response is shown in Figure 9. As shown in Figure 9, skin factor plays a significant role in the early transient flow period. A larger skin factor leads to a higher location of dimensionless pressure and pressure derivative curves. This is because the incremental value of the skin factor results in the increasing additional filtration resistance and the skin effect transition period will last longer. The larger the skin factor is, the slower the pressure wave propagates to the external boundary and the larger the pressure drop is.

4. Conclusions

This paper provided a semianalytical model to investigate the combined effects of dual-permeability flow behavior and stress-dependent fracture permeability on the transient pressure response for a horizontal well in a naturally fractured gas reservoir. The main conclusions of this work are as follows:

(i) A horizontal production well in a naturally fractured gas reservoir with consideration of stress sensitivity effect may exhibit six flow stages: pure wellbore storage stage, skin effect transition stage, early radial flow stage, early linear flow stage, interporosity flow stage, and external boundary response stage

(ii) The stress-dependent fracture permeability imposes effects on the intermediate flow period and the late-time pseudoradial flow period; the existence of dual-permeability flow behavior can make the stress sensitivity effect more significant

(iii) The storability ratio of the fracture, ω_f, mainly affects the duration and the depth of the concave, and a larger ω_f leads to a deeper and wider concave in dimensionless pressure derivative curve. In addition, the storability ratio plays a significant role in the early radial flow stage and early linear flow stage. The interporosity flow factor, λ_{mf}, mainly affects the starting time of the flow exchange from the matrix to the fracture. The larger the value of λ_{mf}, the earlier the occurrence of the interporosity flow period

(iv) The proposed model is suitable for various naturally fractured gas reservoirs and can interpret pressure signals with accurate matching results and more reasonable interpreted parameters

Data Availability

The data used to support the findings of this study are included within the article.

Conflicts of Interest

The authors declare that they have no conflicts of interest.

Acknowledgments

The authors acknowledge that this study was partially funded by the 2021 Innovation and Entrepreneurship Training Projects for College Students in Shanxi Province (no. S202110719144).

References

[1] Y. Wu, L. Cheng, S. Fang, S. Huang, and P. Jia, "A green element method-based discrete fracture model for simulation of the transient flow in heterogeneous fractured porous media," *Advances in Water Resources*, vol. 136, p. 103489, 2020.

[2] P. Jia, L. Cheng, S. Huang, and Y. Wu, "A semi-analytical model for the flow behavior of naturally fractured formations with multi-scale fracture networks," *Journal of Hydrology*, vol. 537, pp. 208–220, 2016.

[3] X. Tian, L. Cheng, R. Cao et al., "A new approach to calculate permeability stress sensitivity in tight sandstone oil reservoirs considering micro-pore-throat structure," *Journal of Petroleum Science and Engineering*, vol. 133, pp. 576–588, 2015.

[4] G. E. Barenblatt, I. P. Zheltov, and I. N. Kochina, "Basic concepts in the theory of seepage of homogeneous liquids in fissured rocks [strata]," *Journal of Applied Mathematics and Mechanics*, vol. 24, no. 5, pp. 1286–1303, 1960.

[5] J. E. Warren and P. J. Root, "The behavior of naturally fractured reservoirs," *SPE Journal*, vol. 3, no. 3, pp. 245–255, 1963.

[6] H. Kazemi, M. S. Seth, and G. W. Thomas, "The interpretation of interference tests in naturally fractured reservoirs with uniform fracture distribution," *SPE Journal*, vol. 9, no. 4, pp. 463–472, 1969.

[7] A. O. De Swaan, "Analytic solutions for determining naturally fractured reservoir properties by well testing," *SPE Journal*, vol. 16, no. 3, pp. 117–122, 1976.

[8] R. Raghavan and C. U. Ohaeri, "Unsteady flow to a well produced at constant pressure in a fractured reservoir," in *SPE California regional meeting*, Bakersfield, California, 1981SPE paper no. SPE-9902-MS.

[9] K. V. Serra, A. C. Reynolds, and R. Raghavan, "New pressure transient analysis methods for naturally fractured reservoirs (includes associated papers 12940 and 13014)," *Journal of Petroleum Technology*, vol. 35, no. 12, pp. 2271–2283, 1983.

[10] Y. Jalali and I. Ershaghi, "Pressure transient analysis of heterogeneous naturally fractured reservoirs," in *SPE California regional meeting*, Ventura, California, 1987SPE paper no. SPE 16341-MS.

[11] Y. Wu and K. Pruess, "A multiple-porosity method for simulation of naturally fractured petroleum reservoirs," *SPE Reservoir Engineering*, vol. 3, no. 1, pp. 327–336, 1988.

[12] T. D. Bui, D. D. Mamora, and W. J. Lee, "Transient pressure analysis for partially penetrating wells in naturally fractured reservoirs," in *SPE rocky mountain regional/low permeability reservoirs symposium and exhibition*, Denver, Colorado, 2000SPE paper no. SPE 60289-MS.

[13] Y. Wu, H. Liu, and G. S. Bodvarsson, "A triple-continuum approach for modeling flow and transport processes in fractured rock," *Journal of Contaminant Hydrology*, vol. 73, no. 1-4, pp. 145–179, 2004.

[14] F. Kuchuk, D. Biryukov, and T. Fitzpatrick, "Fractured-reservoir modeling and interpretation," *SPE Journal*, vol. 20, no. 5, pp. 983–1004, 2015.

[15] S. Wang, L. Cheng, S. Huang et al., "A semi-analytical method for modeling two-phase flow behavior in fractured carbonate oil reservoirs," *Journal of Energy Resources Technology*, vol. 141, no. 7, pp. 072902.1–072902.11, 2019.

[16] B. X. Hu and H. Huang, "Stochastic analysis of reactive solute transport in heterogeneous, fractured porous media: a dual-permeability approach," *Transport in Porous Media*, vol. 48, no. 1, pp. 1–39, 2002.

[17] T. M. Al-Shaalan, L. S. K. Fung, and A. H. Dogru, "A scalable massively parallel dual-porosity dual-permeability simulator for fractured reservoirs with super-k permeability," in *SPE annual technical conference and exhibition*, Denver, Colorado, 2003SPE paper no. SPE 84371-MS.

[18] A. P. G. Van Heel, P. M. Boerrigter, and J. J. Van Dorp, "Thermal and hydraulic matrix-fracture interaction in dual-permeability simulation," *SPE Reservoir Evaluation and Engineering*, vol. 11, no. 4, pp. 735–749, 2008.

[19] L. Jiang, T. Liu, and D. Yang, "A semianalytical model for predicting transient pressure behavior of a hydraulically fractured horizontal well in a naturally fractured reservoir with non-darcy flow and stress-sensitive permeability effects," *SPE Journal*, vol. 24, no. 3, pp. 1322–1341, 2019.

[20] P. Yu, D. Dempsey, and R. Archer, "Techno-economic feasibility of enhanced geothermal systems (EGS) with partially bridging multi-stage fractures for district heating applications," *Energy Conversion and Management*, vol. 257, p. 115405, 2022.

[21] V. Celis, R. Silva, M. Ramones, J. Guerra, and G. da Prat, "A new model for pressure transient analysis in stress sensitive naturally fractured reservoirs," *SPE Advanced Technology*, vol. 2, no. 1, pp. 126–135, 1994.

[22] E. Ozkan, R. Raghavan, and S. D. Joshi, "Horizontal-well pressure analysis," *SPE Formation Evaluation*, vol. 4, no. 4, pp. 567–575, 1989.

[23] E. J. Kuchuk, P. A. Goode, D. J. Wilkinson, and R. K. M. Thambynayagam, "Pressure-transient behavior of horizontal wells with and without gas cap or aquifer," *SPE Formation Evaluation*, vol. 6, no. 1, pp. 86–94, 1991.

[24] A. Hashemi, L. M. Nicolas, and A. C. Gringarten, "Well-test analysis of horizontal wells in gas/condensate reservoirs," *SPE Reservoir Evaluation and Engineering*, vol. 9, no. 1, pp. 86–99, 2006.

[25] R. Nie, Y. Meng, Y. Jia, F. X. Zhang, X. T. Yang, and X. N. Niu, "Dual porosity and dual permeability modeling of horizontal well in naturally fractured reservoir," *Transport in Porous Media*, vol. 92, no. 1, pp. 213–235, 2012.

[26] X. Li, L. Cao, C. Luo, B. Zhang, J. Q. Zhang, and X. H. Tan, "Characteristics of transient production rate performance of horizontal well in fractured tight gas reservoirs with stress-sensitivity effect," *Journal of Petroleum Science and Engineering*, vol. 158, pp. 92–106, 2017.

[27] S. Wang, L. Cheng, Y. Xue et al., "A semi-analytical method for simulating two-phase flow performance of horizontal volatile oil wells in fractured carbonate reservoirs," *Energies*, vol. 11, p. 10, 2018.

[28] Z. Sun, B. Huang, Y. Li, H. Lin, S. Shi, and W. Yu, "Nanoconfined methane flow behavior through realistic organic shale matrix under displacement pressure: a molecular simulation investigation," *Journal of Petroleum Exploration and Production Technologies*, vol. 12, no. 4, 2022.

[29] P. Yu, D. Dempsey, and R. Archer, "A three-dimensional coupled thermo-hydro-mechanical numerical model with partially bridging multi-stage contact fractures in horizontal-well enhanced geothermal system," *International Journal of Rock Mechanics and Mining Sciences*, vol. 143, article 104787, 2021.

[30] Z. Sun, S. Wang, H. Xiong, K. Wu, and J. Shi, "Optimal nanocone geometry for water flow," *AIChE Journal*, vol. 68, no. 3, article e17543, 2022.

[31] O. A. Pedrosa, "Pressure transient response in stress-sensitive formations," in *SPE California regional meeting*, Oakland, California, 1986SPE paper no. SPE-15115-MS.

[32] Stehfest and Harald, "Algorithm 368: numerical inversion of Laplace transforms [D5]," *Communications of the ACM*, vol. 13, no. 1, pp. 47–49, 1970.

[33] F. Kuchuk and Biryukov, "Pressure-transient behavior of continuously and discretely fractured reservoirs," *SPE Reservoir Evaluation and Engineering*, vol. 17, no. 1, pp. 82–97, 2014.